Agricultural Water Management 272 (2022) 107816

Contents lists available at ScienceDirect

Agricultural Water Management

journal homepage: www.elsevier.com/locate/agwat

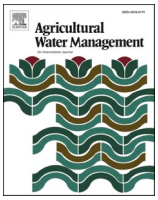

Using LiDAR technique and modified Community Land Model for calculating water interception of cherry tree canopy

Harby Mostafa [b,c], Kowshik K. Saha [a,b], Nikos Tsoulias [b], Manuela Zude-Sasse [b,*]

[a] Technische Universität Berlin, Chair of Agromechatronics, Straße des 17. Juni 135, 10623 Berlin, Germany
[b] Leibniz Institute for Agricultural Engineering and Bioeconomy (ATB), Potsdam, Germany
[c] Agric. and Biosys. Eng. Dept., Faculty of Agriculture, Benha University, Moshtohor, Qalyobia, Egypt

ARTICLE INFO

Handling Editor - Dr R Thompson

Keywords:
Fruit tree
Laser scanner
Leaf area
Leaf area index
Rainfall interception

ABSTRACT

In precision agriculture, methods for analysing 3D point clouds of plants have been introduced, particularly pointing to the high accuracy of light detection and ranging (LiDAR) laser scanning under field conditions. In the present work, LiDAR-based 3D point clouds of cherry trees (n = 255) were analysed for estimating the leaf area as the main factor for water interception. Canopies were scanned for segmenting leaf area pointing to a high variability of canopy surface. The derived tree-specific data of leaf area index (LAI) were implemented into the Community Land Model (CLM), which takes into account canopy interception processes during rainfall events. During canopy development of perennial trees the LAI increased resulting in increased water interception. Events with low rain fall the interception reached 38–100 % capturing LAI of 0.76 – 2.11 m^2/m^2, respectively. In high rainfall events, interception varied 10–14 % capturing the same LAI range. An equation for describing the varying effects of rainfall intensity and LAI is proposed. The evapotranspiration and water interception data point to a substantial decrease of effective water supply that varies tree-individually during the season. In commercial fruit production, the proposed method can support precise irrigation management.

1. Introduction

To mitigate the impact of global warming and drought on the high demand for the limited availability of freshwater resources, irrigation management decisions are critical in arid and semiarid regions. High irrigation water use causes water retention, agricultural nutrient leakage, and reduces water productivity (Afzal et al., 2017). Therefore, precise irrigation scheduling is required to improve crop yield and avoid overwatering.

Tree canopy parameters are involved in key actions of crop management, such as irrigation, but also fertilisation, pesticide application, and crop load management (Zude-Sasse et al., 2016). Canopy features interacting with the environment are the foliage, woody parts, and reproductive organs. Particularly, the leaf area index (LAI) has been introduced for predicting ecosystem models of hydrologic and carbon cycles. Changes in the LAI can affect evapotranspiration (ET), which regulates soil moisture content (Liu et al., 2016; Seo and Kim, 2021). Furthermore, irrigation (Lebon et al., 2006), water stress (Junttila et al., 2021), fertilisation (Rosell and Sanz, 2012), application of plant protection agents (Gil et al., 2014), light interception (Louarn et al., 2008), and fruit yield and quality (Penzel et al., 2021) have all been linked to leaf area and leaf density (Kliewer and Dokoozlian, 2005).

Several models that calculate fluxes among soil and land-surface systems frequently employ the LAI as a key input variable (Gao et al., 2012; Gyeviki et al., 2012; Carrasco-Benavides et al., 2016). The actual LAI is directly measured using time-consuming processes that include partial or complete defoliation of trees. The general effect of foliage enhancing the water interception was shown in deciduous trees (Staelens et al., 2008). However, direct LAI measurements of individual trees in vegetation cover or orchards are hardly applied in large-scale research and are typically used to calibrate indirect methods (Garrigues et al., 2008; Fuentes et al., 2012; Confalonieri et al., 2013). In research, light detection and ranging (LiDAR) laser scanners are frequently employed as an indirect way to analyse trees and arable crops, overcoming effects of varying lighting conditions that limit the use of camera systems (del-Moral-Martínez et al., 2016). The LiDAR sensor is typically mounted on terrestrial or aerial platforms in order to acquire the three-dimensional (3D) profile of plants. Additionally to the LAI, the tree area index (Arnó et al., 2013) as well as the leaf wall area (del-Moral-Martínez et al., 2015) are two further metrics obtained with

* Correspondence to: Leibniz-Institut für Agrartechnik und Bioökonomie e.V. (ATB), Max-Eyth-Allee 100, 14469 Potsdam, Germany
E-mail address: mzude@atb-potsdam.de (M. Zude-Sasse).

https://doi.org/10.1016/j.agwat.2022.107816
Received 14 January 2022; Received in revised form 1 July 2022; Accepted 4 July 2022

terrestrial laser scanners. Recent studies in forestry exploited the potential of 3D point cloud measured for individual tree to discriminate LA from stem area by means of LiDAR backscattered reflectance and geometric features (Hackel et al., 2016, 2022). Using the same method, the estimation of LA was achieved for fruit trees with high accuracy (Zhang et al., 2021; Tsoulias et al., 2022). Similarly, LiDAR backscattered reflectance and geometric features have been exploited to segment cotton balls (Sun et al., 2020) and implemented for autonomous harvesting in greenhouse applications (Tao and Zhou, 2017; Lin et al., 2020). In fruit production, the reflectance intensity and geometric features were combined to identify and segment the total number and size of apples per tree (Gené-Mola et al., 2019; Tsoulias et al., 2020). A similar approach, based on geometric features was introduced to segment 3D points of woody parts from leaves and fruit in pomegranates (Zhang et al., 2021).

Considering irrigation management, LA and LAI play critical roles in hydrological processes. During and after a rain event, leaves intercept substantial amounts of precipitation and evaporate back into the atmosphere. The net intake of orchard soils is determined by taking into account this relationship. Consequently, water resource management requires an understanding of canopy variation in terms of LAI to estimate water interception. Interception is an important component of whole orchards' seasonal water balance, especially in the case of intensive planting systems, where net irrigation requirements should incorporate an estimate of interception loss (Gómez et al., 2001) for precise management. The amount and intensity of rainfall are critical factors in determining canopy interception. In mixed forest, results showed that the canopy of broad-leaved Korean pine intercepted 22 % of rainfall (Sheng and Cai, 2019). However, rainfall interception by the canopy varied from 7 % to 83 %. Interception by olive trees ranged from 7 % to 25 % of the average annual precipitation (606 mm) considering 0.3 and 5.0 m^2/m^2 LAI, respectively (Gómez et al., 2001).

High rainfall amount might lead to changes of canopy interception (Sheng and Cai, 2019; Sun et al., 2011). According to Schneebeli et al. (2012), up to 60 % of rainfall is intercepted during light rainfall, whereas only 4 % is intercepted during periods of strong rainfall, and roughly 15 % of the rain volume is intercepted during rainfalls of medium intensity. Rain interception of oak canopy trees was affected by wind speed (Lockwood and Sellers, 1982). Low wind speeds (0.2 m/s) resulted in no effect on water interception, whereas interception decreased significantly under windy conditions (3.3 m/s) for vinyl trees (Toba and Ohta, 2008). Simulation models such as Community Land Model (CLM) or Gash model have been developed for understanding these important dynamics, because canopy interception can exceed 59 % of yearly precipitation in mature trees (Xiao et al., 2000). Modeling performance was good for olive trees, with total interception loss of 18 % considering the experimental period and modeling using the Gash model (Nóbrega et al., 2015). However, most studies were conducted in forests, whereas in commercial fruit production the CLM hasn't been applied so far. Furthermore, the LA in fruit trees varies within the orchard due to variability in soil properties, planting material, and pruning measures. In deciduous fruit trees, such as sweet cherry production, a seasonal development of foliage takes place, possibly affecting the water interception.

The objectives of this research were (i) to assess the variability of leaf area and LAI in a commercial cherry orchard by means of terrestrial LiDAR laser scanner, and (ii) to construct an empirical model that calculates water interception as a function of cherry LAI and precipitation at individual tree level.

2. Materials and methods

2.1. Study site and field measurement

In Altlandsberg (52.623867 N, 13.816694 E), Brandenburg, Germany, field measurements were carried out in a commercial sweet cherry (*Prunus avium* L. 'Kordia') orchard in 2019. Sweet cherry trees were planted 5 years earlier at a distance of 2 m × 5 m. Except on rainy days, the field was irrigated daily with 4.5 mm using drip irrigation system. A meteorological station (IMT 280, Pessl, Austria) located within the experimental site measured daily precipitation, evapotranspiration, wind speed and direction.

For calculating the water balance according to Penman–Monteith, the reference evapotranspiration (ETo) provided the reference for the crop evapotranspiration (ETc = Kc × ETo), as proposed in FAO-56. The crop coefficient (Kc) showed monthly variability, since it is affected by several factors such as the LA growth. Kc estimated for the condition of an early flowering sweet cherry orchard using the FAO-56 equation. In May and June, the Kc value reached its peak (1.2–1.4). In July, after harvest, the Kc value dropped (0.7–0.8).

2.2. Leaf area measurement and data processing

A two-dimension (2D) LiDAR laser scanner (LMS511 pro model, Sick, Düsseldorf, Germany) mounted on an agricultural tractor with an adjustable rigid aluminium frame served as mobile LiDAR system (MLS). Based on the time-of-flight (ToF) principle, the sensor worked at a wavelength in the near infrared range (905 nm). The MLS included an inertial measurement unit (IMU) (MTi-G-710, XSENS, Enschede, Netherlands) and a real-time kinematic global navigation satellite system (RTK-GNSS) system (AgGPS 542, Trimble, Sunnyvale, USA) for monitoring 3D tilt and georeferencing the laser hits, respectively. The LiDAR laser scanner was mounted on the same frame as the GNSS rover antenna and the IMU. The 2D LiDAR sensor has a field of view (FoV) of 180 degrees, 80 m maximum scanning range, and scanned objects in vertical planes. The tractor was driven at 0.5 km/h along both sides of the rows (n = 255 trees), 1.5 m distance to the centre of the trees (Fig. 1). The mounting height of LiDAR laser scanner (1.6 m) was chosen at half average height of cherry trees, allowing the LiDAR's FoV to capture the full tree from top to bottom. The LiDAR scan was taken with 0.1667° angular resolution, 25 Hz scanning frequency.

Analysis of LiDAR sensor data was carried out according to methodology described previously (Tsoulias et al., 2019; Saha et al., 2020) capturing the merging of the two canopy sides into one 3D point cloud of each tree. Rigid translations and rotations were applied on each point of 3D cloud, while alignment of pairing tree sides was carried out with iterative closest point algorithm, using a k-dimensional space to speed up the process (Vázquez-Arellano et al., 2018; Tsoulias et al., 2019). Segmentation of leaf area (LA) and wood by means of backscattered reflectance and geometric features based on decomposed eigenvalues of covariance matrix (Zhu et al., 2018b; Zhang et al., 2021; Tsoulias et al.,

Fig. 1. The LiDAR sensor, GNSS rover antenna and IMU were installed on a metal frame and mounted on the tractor for scanning of non-defoliated and subsequently defoliated cherry trees at 80 DAFB.

2022). For estimation of LA, the segmented wood was subtracted (Fig. 2) and a linear regression was built considering the segmented LA points and manually measured foliage. Tree canopy scanning was carried out mid of May, June, and July (36, 80, 96 days after bud break [DABB]). The dates were chosen along developmental stages of tree canopy. At 36 DABB, leaves of this season were visible, but not fully grown. Leaves were expanded and mostly mature at 80 DABB and canopy was full-grown at 96 DABB. No further growth can be expected later in the season.

After each of the three LiDAR scans, randomly selected 3, 2, and 2 trees, respectively, were defoliated by hand picking of all leaves collected in plastic bags for reference LA determination. Defoliated trees (n = 7) were scanned again using the LiDAR to calculate the surface area of all stems and branches. To determine the reference LA, all harvested, fresh leaves were scanned from one side in the laboratory with a desktop paper scanner (Scanjet 4850, HP, Palo Alto, CA, USA) in groups of 5–15 leaves to generate RGB-images and all leaves were counted per tree. To calculate the actual LA, a MATLAB script was used to analyse the scanned RGB-images considering the sum of pixels of each leaf (Hobart et al., 2020). The area of 1 cm^2 equalled 6241 pixels, the total area of leaves was determined for each RGB-image of group of leaves.

Increases of LA of individual trees were interpolated with logistic growth model (Tsoulias et al., 2022), where gamma (equ. 1) was adjusted for each individual tree by means of minimising the root mean square error in the fitting process

$$\mathbf{G_{LA}}(t) = (x_{min} \quad x_{max})/(x_{min} + (x_{max}\text{-}x_{min})\ e^{-\gamma t}) \tag{1}$$

where t represented days after bud break; G(t) denotes the estimated growth of LA at t [m^2]; x_{min} was the initial value and x_{max} the upper horizontal asymptote of extracted features and γ was the acceleration and deceleration constant rate of approximation to the two asymptotes.

The surfaces of LA [m^2] obtained from LiDAR scans of the 255 canopies, each on three measuring dates, were further used as index per ground area LAI considering the planting distance of trees.

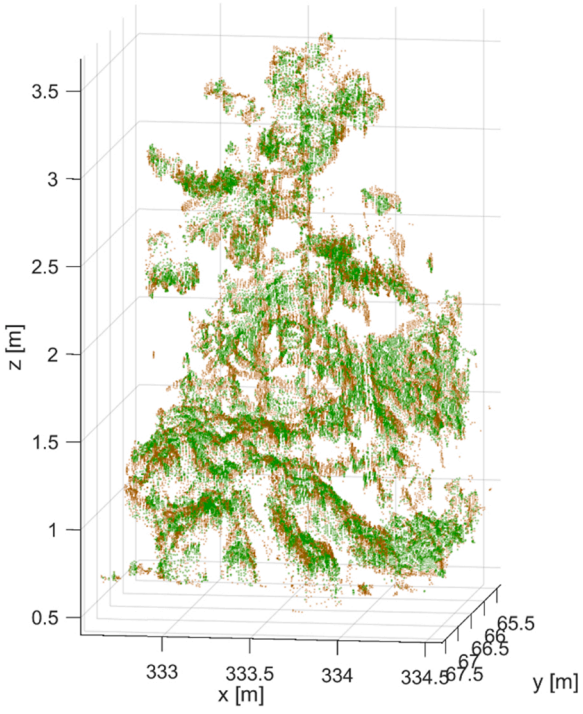

Fig. 2. Registered and aligned 3D point cloud of singularised sweet cherry tree showing the points per tree (PPT) with colour labelling considering the leaf area (green) and wood (brown). The 3D tree point cloud is representative for an average tree found in the orchard.

2.3. Interception calculation

The original canopy interception parameterisation scheme in Community Land Model (CLM4.5) is expressed by Sheng and Cai (2019) as follows:

$$\mathbf{I} = \mathbf{R} \times \quad \boldsymbol{\alpha} \quad [\mathbf{1} - \mathbf{exp}(-\mathbf{0.5} \quad (\mathbf{LAI}))] \tag{2}$$

where I is the intercepted water [%]; α is the empirical parameter (taken as 0.22 according to Yang et al., 2019), R represents the amount of rainfall per day [mm]. In the present study, L (leaf) was replaced by leaf area index, LAI measured with LiDAR laser scanner.

In previous studies, precipitation less than 0.5 mm were considered negligible according to CLM (Sheng and Cai, 2019). Therefore, CLM was modified to consider all rainfall data including the light rainfall events, which provide deeper insight in the influences of canopy surface as follows:

$$\mathbf{I} = \mathbf{m} + \boldsymbol{\alpha} \quad [\mathbf{R} - \mathbf{m}][\mathbf{1} - \mathbf{exp}(-\mathbf{0.5} \quad (\mathbf{LAI}))] \tag{3}$$

where m = R if R < 0.5 and m = 0.4 if R ≥ 0.5.

From the beginning of April (when leaves appeared) through the end of July (fully grown canopy, after harvesting), the rainfall interception was calculated for each day, when precipitation was recorded, considering the tree-individual LAI.

3. Results and discussion

3.1. Estimation of LAI during the canopy growth period

Cherry trees were scanned with LiDAR scanner from both sides, which facilitated to produce a 3D tree point cloud model of each tree (n = 255) at high density of points with average of 109467 points per tree (PPT, Fig. 2). The 3D point clouds were further analysed to segment the leaf area (LA) of the trees. The coefficient of determination for LA estimation based on PPT (LA_{LiDAR}) and manually measured LA (LA_{Manual}) has frequently been reported as very high, also in fruit trees (Pforte et al., 2012; Sanz et al., 2018; Tsoulias et al., 2019; Zhang et al., 2021), which was confirmed in the present study.

However, a limiting factor for the LA_{LiDAR} estimation are occlusion effects occurring in the canopies (Lei et al., 2019) and differences in the percentage of wood during seasonal canopy growth in perennial trees. In the present study, the verification of the LiDAR based LA estimation was carried out considering reference LA_{Manual} analysis (n = 7) after defoliation ranging between 5.7 m^2 and 14.6 m^2 and PPT after removal of points belonging to wood (Fig. 2). A strong correlation (r^2 = 0.93) was found between LiDAR based LA and manually measured LA from the corresponding cherry trees (Fig. 3).

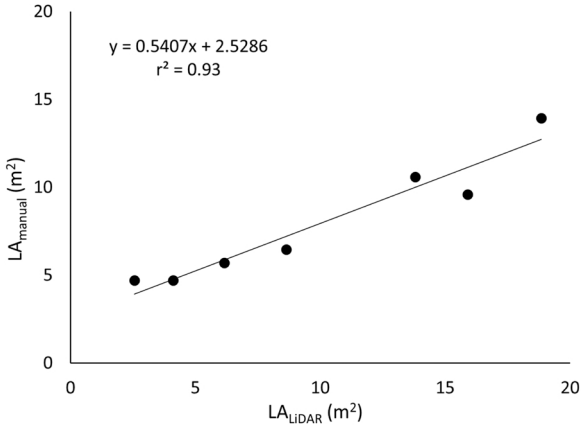

Fig. 3. Scatter plot of leaf area (LA) estimated from LiDAR 3D point cloud and measured destructively after defoliation (n = 7).

Geometric features of linearity and LiDAR backscattered reflectivity were utilised for this purpose as shown earlier, e.g. by Sanz et al. (2018), already revealing high correlation of manual and LiDAR analyses in apples trees (r^2 = 0.88) and vineyards (r^2 = 0.80). Recent work on segmenting woody parts and LA_{LiDAR} at several growth stages in apple trees by means of 3D point cloud analysis, indicated that percentage of wood decreased during canopy growth. Considering the entire vegetation period, LA_{LiDAR} estimation was improved, when subtracting the increased amount of LiDAR points belonging to wood (Tsoulias et al., 2022). The relationship between LA_{Manual} and LA_{LiDAR} were enhanced after removal of woody parts, revealing a substantial increase of $r^2_{adj,\ CV}$ = 0.81 with wood and $r^2_{adj,\ CV}$ = 0.92 without wood (Tsoulias et al., 2022).

The LA_{LiDAR} values obtained at three measuring dates were interpolated by means of growth model (equ. 1) to estimate the G_{LA} of each tree over the season starting at bud break in April until the canopy was fully developed after fruit harvest in July (Fig. 4). During the growth period from 36 days after bud break (DABB) until 80 DABB, the G_{LA} increased sigmoidal as expected. Leaves were developing rapidly till June and with decreased growth rate in July, when the leaves were mature and finally no further canopy growth appeared. Considering all trees (n = 255 per measuring date), LA ranged from 0.02 to 2.95 m^2 in May, 0.15–3.49 m^2 in June, and 0.78–3.51 m^2 in July (Fig. 4).

For further calculation of the canopy water interception, the LA was expressed per unit ground area as dimensionless index LAI. Equally, the LAI changed according to the canopy growth of the perennial, deciduous fruit trees. A high variability of LA and LAI was observed in the orchard, which possibly affects the water interception.

3.2. Effects of rainfall and LAI on canopy water interception

Canopy water interception of rainfall is a dynamic process, thus the interception ratio is not a constant value as reported by Sheng and Cai (2019). Mean interception (%) of all trees at each rain event (31 points) were calculated and the relationship with amount of rainfall described (Fig. 5). An increase of rainfall resulted in exponential decrease of interception (Eq. 4). High coefficient of determination of r^2 = 0.92 was found in the present study. The relationship of rainfall (R) and water interception (I) was calculated as

$$\mathbf{I = 46.958 \quad R^{-0.475}} \tag{4}$$

Rainfall was fully intercepted for light rainfall events less than 0.5 mm (Fig. 5). Mean interception during small rainfall events (< 5 mm) was 42 % compared to 15 % for high rainfall (> 5 mm). During

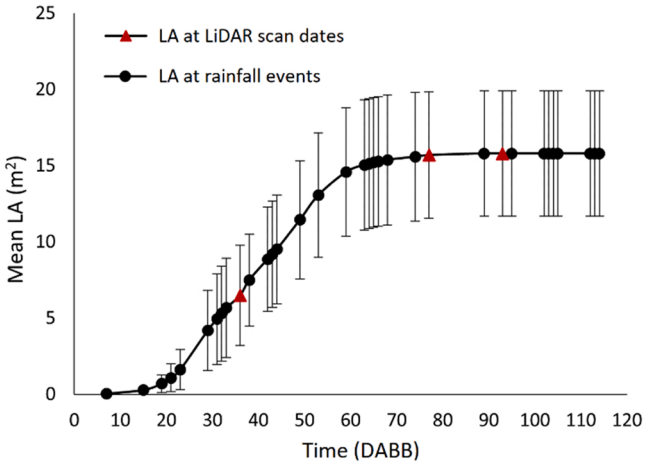

Fig. 4. Mean and standard deviation of leaf area (LA) at rain events (black) calculated for each tree with growth model and LiDAR measurements (red), where LA was directly measured (n = 7905).

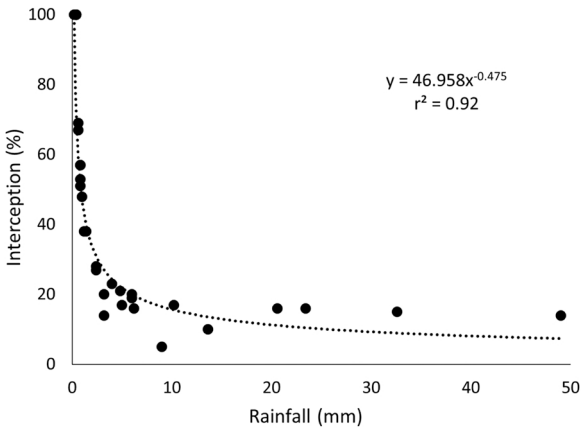

Fig. 5. Water interception considering one mean leaf area index according to the amount of measured rainfall (n = 31).

events with high peak intensities (> 30 mm), calculated interception was occasionally low (14 %). As rainfall continued during most large events (> 30 mm), there was slight difference between gross precipitation and calculated net rainfall as shown earlier (Sidle and Ziegler, 2017; Yerk and Montalto, 2014; Van Stan et al., 2011). Actually, numerous studies have mentioned that the intensity of rain has a significant impact on canopy water interception (Zeng et al., 2000; Murakami, 2007). It was noticed that interception process was sensitive to rainfall intensity, but marginally affected by its duration. With less rainfall intensity, the interception increased because of the proportion of rainwater required for wetting the crown surface, a main component of interception loss from rainfall. In the present study, the maximum calculated interception (100 %) occurred for a rainfall intensity of 0.5 mm/h. In contrast, the minimum interception (5 %) was calculated for a rainfall intensity of 9.0 mm/h.

The mean LAI development generally followed the sigmoid growth curve of LA during the season. However, LiDAR laser scanning of canopies pointed to high variability of LAI of individual trees within the orchard, which can be assumed to affect water interception. Due to the general growth trend of canopies but individual tree growth, this variability of LAI differed at each rain event (Fig. 6).

LAI was calculated for each tree at each rain event considering 255 trees at 31 rainfall events equalling 7905 data sets, which were used in CLM to calculate interception (equ. 2, 3). Changes in canopy surface affected the amount of rainwater intercepted (Fig. 7). However, no trend was visible over the growth period. In May, when the leaves were small, frequently low rainfall events occurred, leading to high percentage of interception. This was the case, even if hardly any LA was measured. On the other hand, in the temperate climate with increased precipitation in summer months, frequently high rainfall event occurred end of June and in July. At these high rainfall events, the percentage of intercepted water decreased even if the foliage was fully developed. Considering the highest rainfall event (23.4 mm) in July, it was found that the water interception of individual trees varied substantially between 9 % and 20 %. The increase of LAI from 1.95 to 2.11 m^2/m^2 during June and July, increased the simulated interception by 6.49 mm (86 %). This was calculated without wind consideration (Lü et al., 2007). However, Toba and Ohta (2008) reported that interception was not significantly affected by low wind speeds (0.2 m/s) and even decreased under windy conditions (3.3 m/s) for vinyl trees.

The relationship of measured rainfall (R) and LAI with estimated water interception (I) was described by one equation (Eq. 5). The coefficient of determination (r^2) between modelled and measured values was high with r^2 = 0.99, and fit standard error and Fstat were found 0.11 and 2736.14, respectively (Fig. 8).

$$\mathbf{I^{-1} = -0.33 + 2.37 \quad / \quad R^{0.5} + 0.97e^{-LAI}} \tag{5}$$

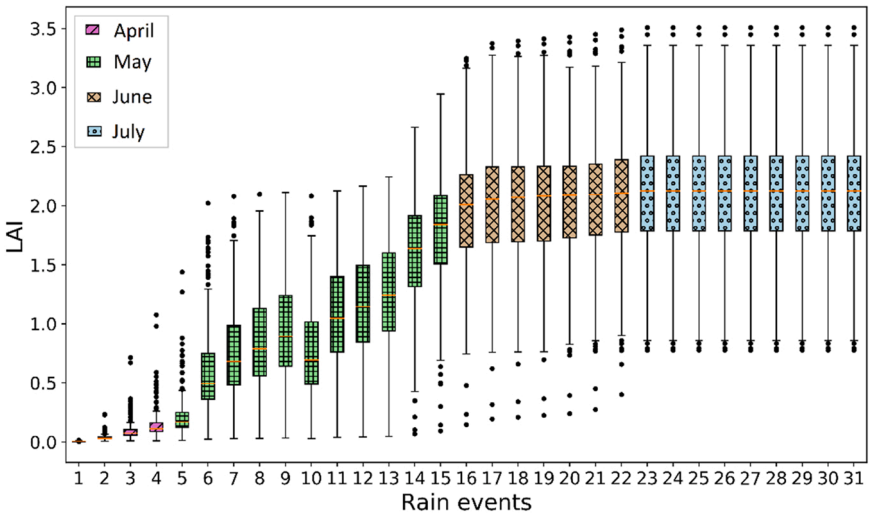

Fig. 6. Box-plot considering leaf area index (LAI) at each rain event (n = 31) in sweet cherry trees (n = 255) in temperate climate in the four months relevant for irrigation resulting in dataset (n = 7905).

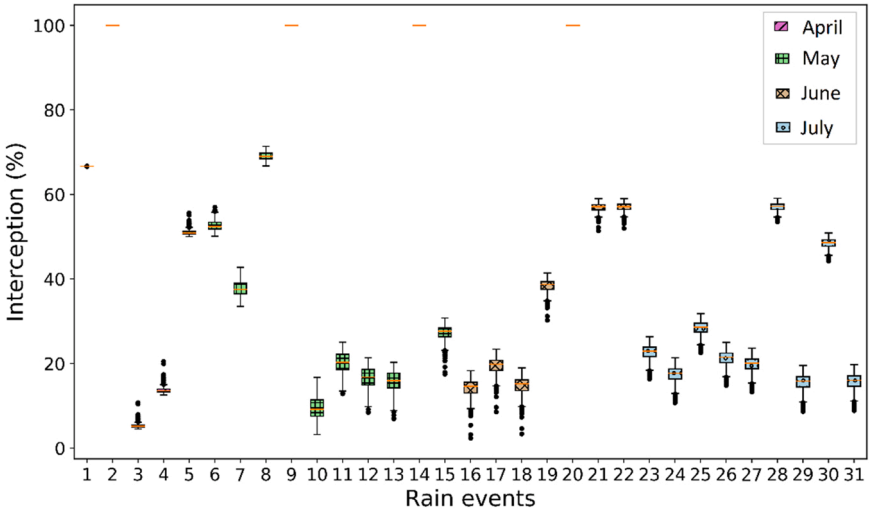

Fig. 7. Box-plot of water interception of cherry tree canopy considering the variation of leaf area index of 255 trees at each rainfall event (n = 7905).

Increasing LAI by 25 % and 50 % resulted in 17 % and 34 % increase in interception. For precise irrigation management in practise, the interception additionally to gross rainfall data would be valuable. Such data can be calculated based on the empirical model. Table 1 presents the summary of calculated interception and gross rainfall for the total of 31 rainfall events in the sweet cherry orchard considering the period from bud break until after harvest, when fruit trees are commonly irrigated in temperate climate. Average interception (%) varied between 27 % and 46 % for the monthly cumulative rainfall depending on LAI. The average interception values for all events was 41 %.

The discrepancy between crop evapotranspiration (ETc) and net rainfall appeared especially in June and July (Fig. 9). The high water needs, here ETc, at high water vapour pressure deficit is the main factor dominating the seasonal trend. The seasonal course of ETc is actually hiding the high variability of percentage of water interception during canopy development. However, despite an increase in rainfall during end of June and in July, water supply is insufficient due to increased water demand. Resulting, from the relationship shown in Fig. 8, in cherry orchard, the interception can be calculated. It can be assumed that the model can be used in other fruit trees as well. The substantial amount of intercepted water explains that it is an important part of the seasonal water balance, and an estimate of water loss due to interception should be factored into the calculation of net irrigation demand. LiDAR laser scanning may, therefore, provide a feasible method for more precise irrigation. Additionally, wind may affect canopy interception (Zabret et al., 2018), especially for medium-size leaves, leathery and smooth such as cherry trees (Gyeviki et al., 2012; Van Stan et al., 2011; Yang et al., 2019), which needs to be investigated further.

4. Conclusion

High spatial resolution information on canopy geometry and structure may result in better orchard management decisions. In this study, LiDAR was applied to estimate LAI as critical parameter influencing rainwater interception by cherry tree canopy in a commercial orchard. The relationship between measured LAI and rainfall with estimated interception was derived from the Community Land Model (CLM), which provides a numerical equation to calculate interception in fruit trees.

The results considering LAI are pointing to inter-tree variability in water interception. As such, the present results support that rainfall interception are increased by increasing LAI and should be considered in seasonal water balance calculations of cherry orchards. The model needs to be confirmed for other fruit trees. Interception losses increase the

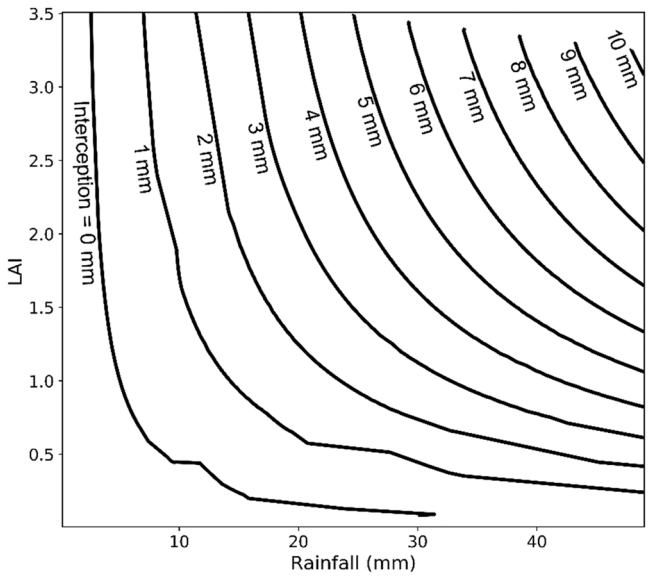

Fig. 8. Relationship between rainfall and water interception considering the leaf area index (LAI) of sweet cherry trees with 255 trees at 31 rainfall event (n = 7905).

Table 1
Monthly interception loss and net rainfall according to LiDAR measurements of the sum of leaf area index (LAI).

Time	No. of rain events	Rainfall (mm)	LAI (m^2/m^2)	Interception (%)
April	4	13.2	0.07 ± 0.09	46.48 ± 38.84
May	11	34.4	1.00 ± 0.06	45.45 ± 31.16
June	7	91.0	2.03 ± 0.57	42.91 ± 28.99
July	9	73.2	2.11 ± 0.55	27.35 ± 14.34
Total	31	211.8	1.30	40.55

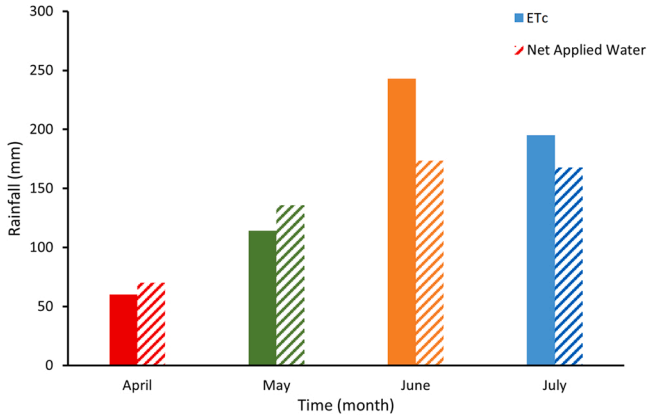

Fig. 9. Monthly crop evapotranspiration and effective precipitation over the period of crop development.

water demand of crops, necessitating additional irrigation demands.

Declaration of Competing Interest

The authors declare that they have no known competing financial interests or personal relationships that could have appeared to influence the work reported in this paper.

Data availability

Data will be made available on request.

Acknowledgements

The first author who funded from the Ministry of Higher Education of the Arab Republic of Egypt would like to present deep gratefulness and appreciation to Benha University, Egypt.

We highly appreciate the financial support by the Bangladesh Agriculture Research Council, Ministry of Agriculture, Bangladesh (PIU BARC, NATP Phase-II Project).

Leibniz Institute for Agricultural Engineering and Bioeconomy (ATB), Germany, for providing the opportunity for this cooperation in the framework of Project IRRIWELL (A novel plant-based approach to estimate irrigation water needs and apply optimal deficit strategy, grant number 01DH21016) funded the investigation through PRIMA initiative of Members States, Associated Countries and Participating Countries. German funding source: BMWK (Bundesministerium für Wirtschaft und Klimaschutz), Berlin; German funding agency: DLR (Deutsche Zentrum für Luft- und Raumfahrt e. V.), Bonn.

References

Afzal, A., Duiker, S.W., Watson, J.E., Luthe, D., 2017. Leaf thickness and electrical capacitance as measures of plant water status. Trans. ASABE 60, 1063–1074. https://doi.org/10.13031/trans.12083.

Arnó, J., Escolà, A., Vallès, J.M., Llorens, J., Sanz, R., Masip, J., Palacín, J., Rosell-Polo, J. R., 2013. Leaf area index estimation in vineyards using a ground-based LiDAR scanner. Precis. Agric. 14, 290–306. https://doi.org/10.1007/s11119-012-9295-0.

Carrasco-Benavides, M., Mora, M., Maldonado, G., Olguín-Cáceres, J., von Bennewitz, E., Ortega-Farías, S., Gajardo, J., Fuentes, S., 2016. Assessment of an automated digital method to estimate leaf area index (LAI) in cherry trees. N. Z. J. Crop Hortic. Sci. 44, 247–261. https://doi.org/10.1080/01140671.2016.1207670.

Confalonieri, R., Foi, M., Casa, R., Aquaro, S., Tona, E., Peterle, M., Boldini, A., De Carli, G., Ferrari, A., Finotto, G., Guarneri, T., Manzoni, V., Movedi, E., Nisoli, A., Paleari, L., Radici, I., Suardi, M., Veronesi, D., Bregaglio, S., Cappelli, G., Chiodini, M.E., Dominoni, P., Francone, C., Frasso, N., Stella, T., Acutis, M., 2013. Development of an app for estimating leaf area index using a smartphone. Trueness and precision determination and comparison with other indirect methods. Comput. Electron. Agric. 96, 67–74. https://doi.org/10.1016/j.compag.2013.04.019.

del-Moral-Martínez, I., Arnó, J., Escolà, A., Sanz, R., Masip-Vilalta, J., Company-Messa, J., Rosell-Polo, J., 2015. Georeferenced scanning system to estimate the leaf wall area in tree crops. Sensors 15, 8382–8405. https://doi.org/10.3390/s150408382.

del-Moral-Martínez, I., Rosell-Polo, J., Company, J., Sanz, R., Escolà, A., Masip, J., Martínez-Casasnovas, J., Arnó, J., 2016. Mapping vineyard leaf area using mobile terrestrial laser scanners: should rows be scanned on-the-go or discontinuously sampled? Sensors 16, 119. https://doi.org/10.3390/s16010119.

Fuentes, S., Bei, Rd, Pozo, C., Tyerman, S., 2012. Development of a smartphone application to characterise temporal and spatial canopy architecture and leaf area index for grapevines. Wine Vitic. J. 27, 56–60.

Gao, F., Anderson, M., Kustas, W., Wang, Y., 2012. Simple method for retrieving leaf area index from Landsat using MODIS leaf area index products as reference. J. Appl. Remote Sens. 6, 063554 https://doi.org/10.1117/1.JRS.6.063554.

Garrigues, S., Shabanov, N.V., Swanson, K., Morisette, J.T., Baret, F., Myneni, R.B., 2008. Intercomparison and sensitivity analysis of Leaf Area Index retrievals from LAI-2000, AccuPAR, and digital hemispherical photography over croplands. Agric. For. Meteorol. 148, 1193–1209. https://doi.org/10.1016/j.agrformet.2008.02.014.

Gené-Mola, J., Gregorio, E., Guevara, J., Auat, F., Sanz-Cortiella, R., Escolà, A., Llorens, J., Morros, J.-R., Ruiz-Hidalgo, J., Vilaplana, V., Rosell-Polo, J.R., 2019. Fruit detection in an apple orchard using a mobile terrestrial laser scanner. Biosyst. Eng. 187, 171–184. https://doi.org/10.1016/j.biosystemseng.2019.08.017.

Gil, E., Arnó, J., Llorens, J., Sanz, R., Llop, J., Rosell-Polo, J., Gallart, M., Escolà, A., 2014. Advanced technologies for the improvement of spray application techniques in Spanish viticulture: an overview. Sensors 14, 691–708. https://doi.org/10.3390/s140100691.

Gómez, J.A., Giráldez, J.V., Fereres, E., 2001. Rainfall interception by olive trees in relation to leaf area. Agric. Water Manag. 49, 65–76. https://doi.org/10.1016/S0378-3774(00)00116-5.

Gyeviki, M., Hrotkó, K., Honfi, P., 2012. Comparison of leaf population of sweet cherry (Prunus avium L.) trees on different rootstocks. Sci. Hortic. 141, 30–36. https://doi.org/10.1016/j.scienta.2012.03.015.

Hackel, T., Wegner, J.D., Schindler, K., 2016. Contour detection in unstructured 3D point clouds. In: Proceedings of the IEEE Conference on Computer Vision and Pattern Recognition (CVPR). IEEE, Las Vegas, NV, USA, 2016, 1610–1618. ⟨https://doi.org/10.1109/cvpr.2016.178⟩.

Hobart, M., Pflanz, M., Weltzien, C., Schirrmann, M., 2020. Growth height determination of tree walls for precise monitoring in apple fruit production using UAV photogrammetry. Remote Sens. 12, 1656. https://doi.org/10.3390/rs12101656.

Junttila, S., Hölttä, T., Puttonen, E., Katoh, M., Vastaranta, M., Kaartinen, H., Holopainen, M., Hyyppä, H., 2021. Terrestrial laser scanning intensity captures diurnal variation in leaf water potential. Remote Sens. Environ. 255, 112274 https://doi.org/10.1016/j.rse.2020.112274.

Kliewer, W.M., Dokoozlian, N.K., 2005. Leaf area/crop weight ratios of grapevines: influence on fruit composition and wine quality. Am. J. Enol. Viticult., 56, 170-181. ⟨https://www.ajevonline.org/content/ajev/56/2/170.full.pdf⟩. (Accessed 3 August 2022).

Lebon, E., Pellegrino, A., Louarn, G., Lecoeur, J., 2006. Branch development controls leaf area dynamics in grapevine (Vitis vinifera) growing in drying soil. Ann. Bot. 98, 175–185. https://doi.org/10.1093/aob/mcl085.

Lei, L., Qiu, C., Li, Z., Han, D., Han, L., Zhu, Y., Wu, J., Xu, B., Feng, H., Yang, H., Yang, G., 2019. Effect of leaf occlusion on leaf area index inversion of maize using UAV–LiDAR data. Remote Sens. 11, 1067. https://doi.org/10.3390/rs11091067.

Lin, G., Tang, Y., Zou, X., Xiong, J., Fang, Y., 2020. Color-, depth-, and shape-based 3D fruit detection. Precis. Agric. 21, 1–17. https://doi.org/10.1007/s11119-019-09654-w.

Liu, L., Zhang, R., Zuo, Z., 2016. The relationship between soil moisture and LAI in different types of soil in central Eastern China. J. Hydrometeorol. 17, 2733–2742. https://doi.org/10.1175/jhm-d-15-0240.1.

Lockwood, J.G., Sellers, P.J., 1982. Comparisons of interception loss from tropical and temperate vegetation canopies. J. Appl. Meteorol. (1962-1982) 21, 1405–1412. ⟨http://www.jstor.org/stable/26180757⟩ (Accessed 3 August 2022).

Louarn, G., Lecoeur, J., Lebon, E., 2008. A three-dimensional statistical reconstruction model of grapevine (Vitis vinifera) simulating canopy structure variability within and between cultivar/training system Pairs. Ann. Bot. 101, 1167–1184. https://doi.org/10.1093/aob/mcm170.

Lü, Y., Liu, S., Sun, P., Liu, X., Zhang, R., 2007. Canopy interception of sub-alpine dark coniferous communities in western Sichuan, China. J. Appl. Ecol. 18, 2398–2405.

Murakami, S., 2007. Application of three canopy interception models to a young stand of Japanese cypress and interpretation in terms of interception mechanism. J. Hydrol. 342, 305–319. https://doi.org/10.1016/j.jhydrol.2007.05.032.

Nóbrega, C., Pereira, F.L., Valente, F., 2015. Measuring and modelling interception loss by an isolated olive tree in a traditional olive grove - pasture system, EGU General Assembly 2015, Vienna, Austria, 7765. ⟨https://meetingorganizer.copernicus.org/EGU2015/EGU2015–7765.pdf⟩. (Accessed 3 August 2022).

Penzel, M., Herppich, W.B., Weltzien, C., Tsoulias, N., Zude-Sasse, M., 2021. Modeling of individual fruit-bearing capacity of trees is aimed at optimizing fruit quality of Malus x domestica Borkh. 'Gala'. Front. Plant Sci. 12. https://doi.org/10.3389/fpls.2021.669909.

Pforte, F., Selbeck, J., Hensel, O., 2012. Comparison of two different measurement techniques for automated determination of plum tree canopy cover. Biosyst. Eng. 113, 325–333. https://doi.org/10.1016/j.biosystemseng.2012.09.014.

Rosell, J.R., Sanz, R., 2012. A review of methods and applications of the geometric characterization of tree crops in agricultural activities. Comput. Electron. Agric. 81, 124–141. https://doi.org/10.1016/j.compag.2011.09.007.

Saha, K.K., Tsoulias, N., Zude-Sasse, M., 2020. Assessment of measurement uncertainty when using 2D mobile laser scanner to estimate tree parameters. Agric. Eng. 75. https://doi.org/10.15150/lt.2020.3251.

Sanz, R., Llorens, J., Escolà, A., Arnó, J., Planas, S., Román, C., Rosell-Polo, J.R., 2018. LIDAR and non-LIDAR-based canopy parameters to estimate the leaf area in fruit trees and vineyard. Agric. For. Meteorol. 260–261, 229–239. https://doi.org/10.1016/j.agrformet.2018.06.017.

Schneebeli, M., Wolf, S., Kunert, N., Eugster, W., Mätzler, C., 2012. Time series of canopy intercepted water and dew observed in a tropical tree plantation by means of microwave radiometry, EGU General Assembly 2012, Vienna, Austria, 4055. ⟨https://meetingorganizer.copernicus.org/EGU2012/EGU2012–4055-1.pdf⟩. (Accessed 3 August 2022).

Seo, H., Kim, Y., 2021. Role of remotely sensed leaf area index assimilation in eco-hydrologic processes in different ecosystems over East Asia with Community Land Model version 4.5 – Biogeochemistry. J. Hydrol. 594, 125957 https://doi.org/10.1016/j.jhydrol.2021.125957.

Sheng, H., Cai, T., 2019. Influence of Rainfall on Canopy Interception in Mixed Broad-Leaved—Korean Pine Forest in Xiaoxing'an Mountains, Northeastern China. Forests 10, 248. https://doi.org/10.3390/f10030248.

Sidle, R.C., Ziegler, A.D., 2017. The canopy interception–landslide initiation conundrum: insight from a tropical secondary forest in northern Thailand. Hydrol. Earth Syst. Sci. 21, 651–667. https://doi.org/10.5194/hess-21-651-2017.

Staelens, J., De Schrijver, A., Verheyen, K., Verhoest, N.E.C., 2008. Rainfall partitioning into throughfall, stemflow, and interception within a single beech (Fagus sylvatica L.) canopy: influence of foliation, rain event characteristics, and meteorology. Hydrol. Process. 22, 33–45. https://doi.org/10.1002/hyp.6610.

Sun, S., Li, C., Chee, P.W., Paterson, A.H., Jiang, Y., Xu, R., Robertson, J.S., Adhikari, J., Shehzad, T., 2020. Three-dimensional photogrammetric mapping of cotton bolls in situ based on point cloud segmentation and clustering. ISPRS J. Photogramm. Remote Sens. 160, 195–207. https://doi.org/10.1016/j.isprsjprs.2019.12.011.

Sun, X.Y., Wang, G.X., Li, W., Liu, G.S., Lin, Y., 2011. Measurements and modeling of canopy interception in the Gongga Mountain subalpine succession forest. Adv. Water Sci. 22, 23–29. ⟨http://skxjz.nhri.cn/en/article/id/1776⟩ (Accessed 3 August 2022).

Tao, Y., Zhou, J., 2017. Automatic apple recognition based on the fusion of color and 3D feature for robotic fruit picking. Comput. Electron. Agric. 142, 388–396. https://doi.org/10.1016/j.compag.2017.09.019.

Toba, T., Ohta, T., 2008. Factors affecting rainfall interception determined by a forest simulator and numerical model. Hydrol. Process. 22, 2634–2643. https://doi.org/10.1002/hyp.6859.

Tsoulias, N., Paraforos, D.S., Fountas, S., Zude-Sasse, M., 2019. Estimating canopy parameters based on the stem position in apple trees using a 2D LiDAR. Agronomy 9, 740. https://doi.org/10.3390/agronomy9110740.

Tsoulias, N., Paraforos, D.S., Xanthopoulos, G., Zude-Sasse, M., 2020. Apple shape detection based on geometric and radiometric features using a LiDAR laser scanner. Remote Sens. 12, 2481. https://doi.org/10.3390/rs12152481.

Tsoulias, N., Xanthopoulos, G., Fountas, S., Zude-Sasse, M., 2022. Effects of soil ECa and LiDAR-derived leaf area on yield and fruit quality in apple production. Biosyst. Eng. https://doi.org/10.1016/j.biosystemseng.2022.03.007.

Van Stan II, J.T., Siegert, C.M., Levia, D.F., Scheick, C.E., 2011. Effects of wind-driven rainfall on stemflow generation between codominant tree species with differing crown characteristics. Agric. For. Meteorol. 151, 1277–1286. https://doi.org/10.1016/j.agrformet.2011.05.008.

Vázquez-Arellano, M., Reiser, D., Paraforos, D.S., Garrido-Izard, M., Burce, M.E.C., Griepentrog, H.W., 2018. 3-D reconstruction of maize plants using a time-of-flight camera. Comput. Electron. Agric. 145, 235–247. https://doi.org/10.1016/j.compag.2018.01.002.

Xiao, Q., McPherson, E.G., Ustin, S.L., Grismer, M.E., 2000. A new approach to modeling tree rainfall interception. J. Geophys. Res. Atmos. 105, 29173–29188. https://doi.org/10.1029/2000jd900343.

Yang, M., Zuo, R., Li, X., Wang, L., 2019. Improvement test for the canopy interception parameterization scheme in the community land model. Sola 15, 166–171. https://doi.org/10.2151/sola.2019-030.

Yerk, W., Montalto, F., 2014. Quantifying dominance of intra-storm phase of interception process by small isolated canopies, EGU General Assembly 2014, Vienna, Austria, 13324. ⟨https://meetingorganizer.copernicus.org/EGU2014/EGU2014–13324-7.pdf⟩. (Accessed 3 August 2022).

Zabret, K., Rakovec, J., Šraj, M., 2018. Influence of meteorological variables on rainfall partitioning for deciduous and coniferous tree species in urban area. J. Hydrol. 558, 29–41. https://doi.org/10.1016/j.jhydrol.2018.01.025.

Zeng, N., Shuttleworth, J.W., Gash, J.H.C., 2000. Influence of temporal variability of rainfall on interception loss. Part I. Point analysis. J. Hydrol. 228, 228–241. https://doi.org/10.1016/s0022-1694(00)00140-2.

Zhang, C., Zhang, K., Ge, L., Zou, K., Wang, S., Zhang, J., Li, W., 2021. A method for organs classification and fruit counting on pomegranate trees based on multi-features fusion and support vector machine by 3D point cloud. Sci. Hortic. 278, 109791 https://doi.org/10.1016/j.scienta.2020.109791.

Zhu, X., Skidmore, A.K., Darvishzadeh, R., Niemann, K.O., Liu, J., Shi, Y., Wang, T., 2018a. Foliar and woody materials discriminated using terrestrial LiDAR in a mixed natural forest. Int. J. Appl. Earth Obs. Geoinf. 64, 43–50. https://doi.org/10.1016/j.jag.2017.09.004.

Zhu, X., Skidmore, A.K., Wang, T., Liu, J., Darvishzadeh, R., Shi, Y., Premier, J., Heurich, M., 2018b. Improving leaf area index (LAI) estimation by correcting for clumping and woody effects using terrestrial laser scanning. Agric. For. Meteorol. 263, 276–286. https://doi.org/10.1016/j.agrformet.2018.08.026.

Zude-Sasse, M., Fountas, S., Gemtos, T.A., Abu-Khalaf, N., 2016. Applications of precision agriculture in horticultural crops. Eur. J. Hortic. Sci. 81, 78–90. https://doi.org/10.17660/eJHS.2016/81.2.2.